Received Date:28th December, 2023
Revision Date:18th June, 2024
Accepted Date:12th July, 2024

Modeling of Grid Tied PV Inverter to Improve its Performance During Unbalanced Load and Unbalance Fault

Bibek Khanal[1*], Kulchandra Bhattarai[2], Lenish Shrestha[3], Aashish Dahal[4], Indraman Tamrakar[5]

[1]Dept. of Electrical Engineering, Pulchowk Campus, IOE, TU. Email : 075bel011.bibek@pcampus.edu.np
[2]Dept. of Electrical Engineering, Pulchowk Campus, IOE, TU. Email : 075bel021.kulchandra@pcampus.edu.np
[3]Dept. of Electrical Engineering, Pulchowk Campus, IOE, TU. Email : 075bel022.lenish@pcampus.edu.np
[4]Dept. of Electrical Engineering, Pulchowk Campus, IOE, TU. Email : 075bel003.aashish@pcampus.edu.np
[5]Professor, Dept. of Electrical Engineering, Pulchowk Campus, IOE, TU. Email : imtamrakar@ioe.edu.np

***Abstract*—Integrating solar through inverter brings about various challenges in the microgrids and the inverter itself. This paper aims to the study of problems in the operation of inverter during unbalance load and unbalance fault condition along with the possible control measures to mitigate those problems to ensure the safe and reliable operation of the inverter. A grid connected PV inverter is modeled using hysteresis band controller and implementing the MPPT of the PV system with the buck boost converter. During unbalance load and unbalance fault condition, the negative and zero sequence components of current exists. All the zero-sequence component of current is delivered by the grid. The negative sequence component of current also flows through the inverter resulting in high value of current and loss of stability. Also, the voltage across the dc link capacitor increases during fault. The high value of current flowing through the inverter and high voltage across dc link capacitor may damages the inverter and capacitor respectively. An inverter dual current controller is introduced replacing the hysteresis band control such that the negative sequence component of current flowing through the inverter is almost mitigated from 600A to 10A and positive sequence current is also reduced relatively to a tolerable value 150A from 550A. The total current flowing through the inverter is limited to 200A from 950A and voltage across dc link capacitor is limited to 700V from 1050V during LG fault at the inverter side thus ensuring safe operation of the inverter during voltage dip condition. A further study can be done on limiting the positive sequence component of current to a rated value and improving the performance while operating in islanded mode.**

Keywords- Photovoltaic System (PV); solar irradiance; Maximum Power Point Tracking (MPPT); inverter current; voltage across dc link capacitor; sequence components of current; Dual Second Order Generalized Integrator (DSOGI)

Introduction

With the demand of alternative source of energy, there is an increasing trend in solar power plants due to their reliability, less carbon emission and cost effectiveness however their intermittency and environment dependent factor affects the efficiency. The overall efficiency and the performance of the solar PV can be enhanced by integration with the utility grid through dc-dc converter and the inverterr [1]. To address the nonlinear behaviour of PV, the tracking of maximum power under changing environmental conditions is crucial to achieve optimum power outputt [2]. The various MPPT techniques such as FOCV [3], FSCC [4], CF [4], HC [5], INC [6], etc. have been used. These approaches differ in terms of their implementation, cost, speed, and efficiency.

Zhong et al. [7], used a droop control in the three-phase three-leg inverter connecting the number of solar to the grid but limited to balanced condition. However, the grid has to supply both single phase and three phase loads causing the voltage of the inverter to be unbalanced [8]. The existence of negative and zero sequence components of current due unbalance load and unbalance fault causes increase in the current flowing through the inverter, large double frequency current/voltage ripples on the dc link [9], increase in the Third Harmonic Distortion (THD) [10] and hence degrades the power quality of the system [11] thereby the conventional droop control is difficult to realize [12].

Bases on grid codes [13], PV inverters should be connected to the grid during voltage dip conditions caused by the unbalance load and unbalance fault so the compensation of the negative and zero sequence components of the current is necessary. Fang et al. [12], proposed an advanced droop control where the sequence components of currents are controlled by the virtual impedance method in addition to conventional droop control. In [14], Active Power Filters (APFs) is used for compensating the load unbalances and harmonics caused by negative sequence current. Several control algorithms such as adaptive shunt filtering control [15], model reference adaptive system [16] and adaptive observer-based control [17] have been used for controlling

* *Corresponding Author*

positive and negative sequence current but it doesn't consider the zero-sequence current. Jiang and Shang [18], presents four leg inverter topologies where positive and negative sequence current is controlled using the fourth leg. Alternatively, the zero-sequence current can also be controlled in three- leg inverter with a D-Y transformer [19] or zigzag transformer [20] but it is heavy and costly. Chen et al. [21], proposed the Dual Vector Current Control method to limit the ripple power and peak currents. This paper proposes a dual current controller method, utilizing the DSOGI method for extracting sequence components of both voltage and current. The current reference generation is optimized to limit current and reduce DC-link voltage oscillations. For the effectiveness of this controller a standalone PV system is demonstrated through MATLAB simulations.

Methodology

A. Selection of PV Panel

The PV panel is selected in the MATLAB Simulink as per the following table.

TABLE 1

PV SPECIFICATION

Components used	1 Soltech 1STH – 215 – P
Maximum Power	213.5 W
Open Circuit Voltage (V_{OC})	36.3 V
Short Circuit Current (I_{SC})	7.35 A
Parallel strings	11
Series-connected modules per string	22
Total open circuit voltage	36.3 * 22 = 798.6 V
Total maximum Power	22*11*213.5 = 51.667 KW

B. Grid connected PV System Using Hysteresis Band Controller

The grid connected PV system using hysteresis band controller is modeled in MATLAB Simulink to study the effect of unbalance load and unbalance fault.

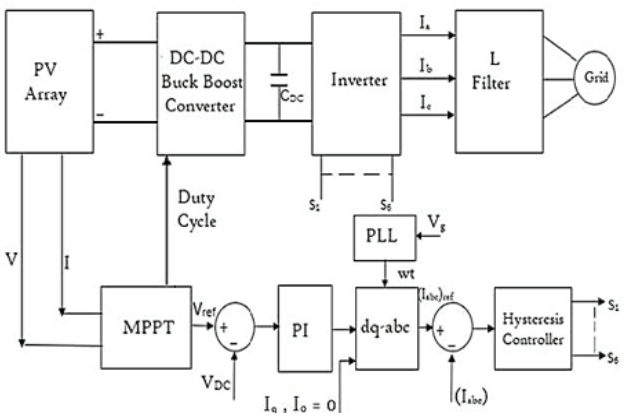

Fig 1 Block diagram of grid connected PV system

Fig.1 shows the block diagram of Grid Connected PV System. The PV Array is connected to the inverter through buck boost converter to maintain the maximum power. To ensure maximum power tracking, it is crucial for the PV system to operate at the voltage that corresponds to the maximum power point. While a boost converter can be an option, it becomes ineffective when the PV voltage exceeds the maximum power voltage, requiring voltage reduction. However, this case is equivalent to open circuit condition which is rare during operating condition. So, for the efficient operation, a buck boost converter is used. The voltage across the PV and current flowing through the PV are sent to the MPPT which uses the P & O algorithm to generate a duty cycle that controls the operation of buck boost converter such that the PV works at the voltage corresponding to the maximum power. The voltage generated by the MPPT block is compared with the dc link capacitor voltage then uses PI controller to generate the reference d component of current. And then keeping the component zero as there is no consideration of reactive power, the 3-φ current reference is generated using dq - abc conversion. PLL block is used to generate the frequency of grid which is required for dq - abc conversion. The reference current is compared with the actual current flowing through the inverter to get the PWM signal to control switching operation of the IGBT's used in the inverter.

C. Sequence Components Extraction

The initial step of dual current control method involves extracting of positive and negative sequence components. For this work, DSOGI method has been applied, which integrates the QSG along with calculations for +ve and -ve sequence component. DSOGI method has advantages in terms of accuracy, speed, and adaptability to varying frequencies improving the overall controller performance. Moreover, it acts as a bandpass filter (BPF) by effectively rejecting higher-order switching frequencies [22].

The stationary voltages are transformed into two components that are orthogonal to each other, differing by 90 degrees [22]. The transfer function of the SOGI-QSG scheme is:

$$D(s) = \frac{V'}{V}(S) = \frac{K w' s}{s^2 + k w' s + w'^2} \quad (1)$$

$$Q(s) = \frac{qV'}{V}(S) = \frac{K w'^2}{s^2 + k w' s + w'^2} \quad (2)$$

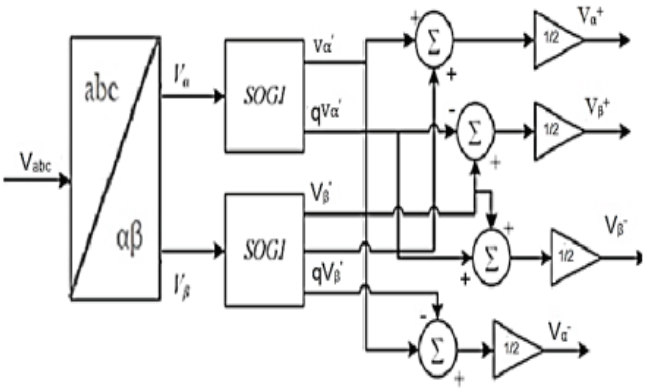

Fig 2 Block diagram for extraction of sequence components of current using DSOGI

Fig. 2 shows the block diagram for sequence components extraction. The voltage is converted into sequence components in αβ voltages through an arithmetic calculation, commonly referred to as the sequence calculator, as demonstrated below.

$$V_{\alpha}^{+} = \frac{V\alpha' + qV\beta'}{2} \quad (3)$$

$$V_{\alpha}^{-} = \frac{V\alpha' - qV\beta'}{2} \quad (4)$$

$$V_{\beta}^{+} = \frac{V\beta' - qV\alpha'}{2} \quad (5)$$

$$V_{\beta}^{-} = \frac{qV\alpha + V\beta'}{2} \quad (6)$$

D. Inverter Dual Current Control

Inverter dual current control is used as a replacement for hysteresis band control to control the sequence components of current limiting the current flowing through the inverter to a safer value.

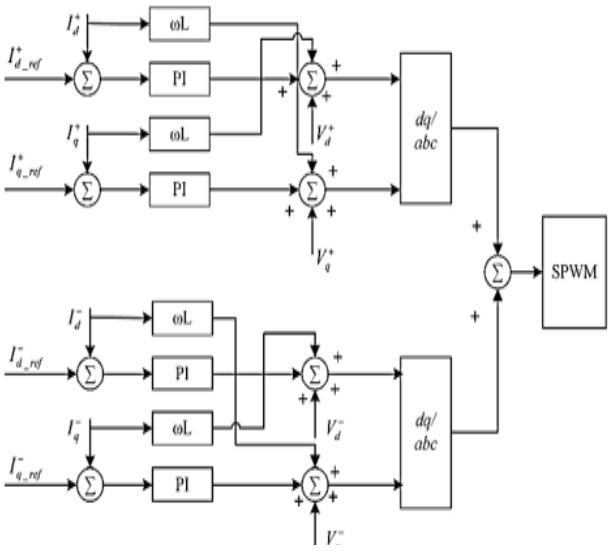

Fig 3 Inverter dual current control

Fig. 3 depicts the control design of the inverter used in this study. In order to regulate specific system states, a conventional PI controller is employed, utilizing proportional gain and integrator components. The PI controller receives the error from tracking the positive and negative reference current. Next, the feed-forward voltage is merged with the corresponding voltage calculation, resulting in the generation of commanded voltages for the d-axis and q-axis according to the given equation:

$$U_d = (K_p + \frac{Ki}{s})(i_d^* - i_d) - wLi_{q+}V_d \quad (7)$$

$$U_q = (K_p + \frac{Ki}{s})(i_q^* - i_q) - wLi_{d+}V_q \quad (8)$$

The voltages U_d and U_q are initially expressed in the terms of d-q components, and it is necessary to convert them into stationary reference frame i.e., abc voltages using the conversion process from dq to αβ accomplished using equation shown below [22].

$$\begin{pmatrix} V\alpha \\ V\beta \end{pmatrix} = \begin{pmatrix} sin\theta & cos\theta \\ cos\theta & -sin\theta \end{pmatrix} = \begin{pmatrix} Vd \\ Vq \end{pmatrix} \quad (9)$$

E. Overall Simulink Model

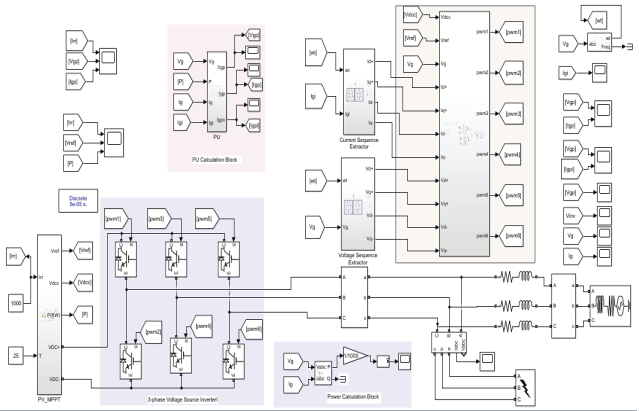

Fig 4 Overall simulink model of grid connected PV system using inverter dual current control

Fig. 4 shows the overall Simulink model of grid connected PV system using inverter dual current control mechanism. The PV_MPPT subsystem consists of the PV panel followed by the buck boost converter along with the implementation of MPPT algorithm thus maintaining the voltage of the PV panel and dc link capacitor corresponding to the maximum power at varying irradiances. The output of buck boost converter is then fed as an input to the three phase VSI and then connected to the utility grid through L filter. A LG fault is given at the output side of the inverter and various parameters such as current and voltages at various points are measured to observe the results. The voltage sequence extractor and the current sequence extractor subsystem splits the grid voltage and current flowing through the

inverter in terms of their sequence components respectively using DSOGI method and fed as an input to the current controller subsystem. The current controller then compares the sequence components of current and voltage with their reference values and a reference current to be flowed through the inverter is obtained using inverter dual current control method. Thus, obtained reference current uses the sinusoidal pulse width modulation technique to generate the control gate signals to control the switching operation of the inverter.

Simulation Results

A. Problem Study

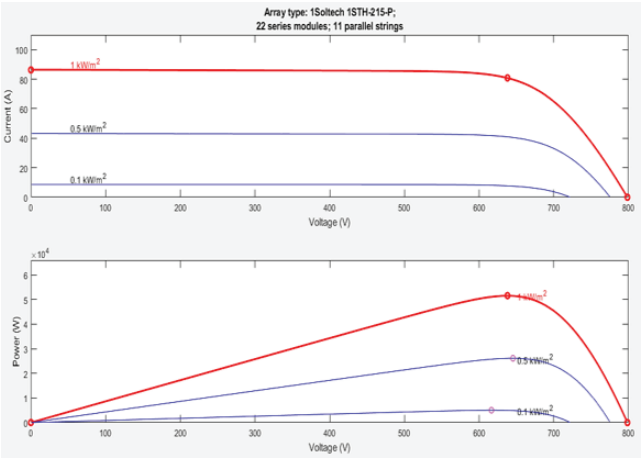

Fig 5 I-V and P-V characteristics of PV system at different irradiance level

Fig. 5 shows the I-V and P-V characteristics of the selected PV array. From the figure the current and power variation with respect to voltage level can be observed at different irradiance level. The maximum power point for different irradiance level can also be observed along with the corresponding voltage level. The voltage level for maximum power and the maximum power varies according to irradiance level.

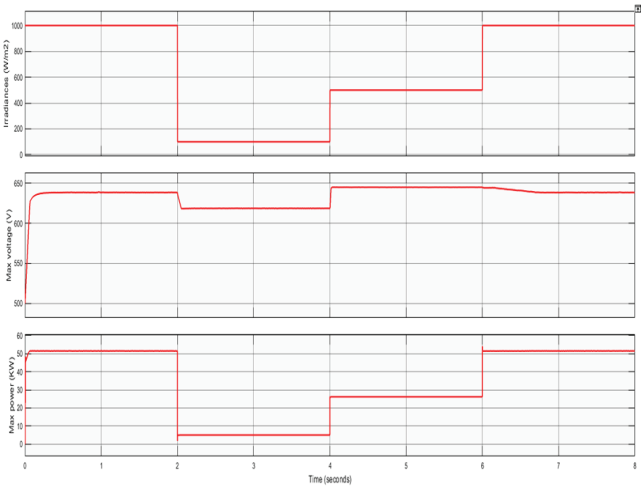

Fig 6 MPPT demonstration

Fig. 6 demonstrates the MPPT system at work as the PV system power delivery and corresponding voltage level for maximum power point is tracked by the MPPT. We can see that at 1000 w/m2 irradiance the power delivered is maximum i.e., around 51KW and respective voltage is around 638 V. Similarly, the voltage level corresponding to maximum power is tracked at the output of PV terminal despite of the change in irradiance thus delivering maximum power at all varying irradiance.

- *Theoretical current value*

For 1 KW/m2 irradiances, P= 51.58 kw

Then, max per phase peak current $= \frac{51.58 \times 1000}{3 \times \frac{400}{\sqrt{3}}} \times \sqrt{2}$

$= 105.28$ A

Similarly,

For 500 W/m2 irradiances, P= 26.13 kw

Then, max per phase peak current $= \frac{26.13 \times 1000}{3 \times \frac{400}{\sqrt{3}}} \times \sqrt{2}$

$= 53.33$ A

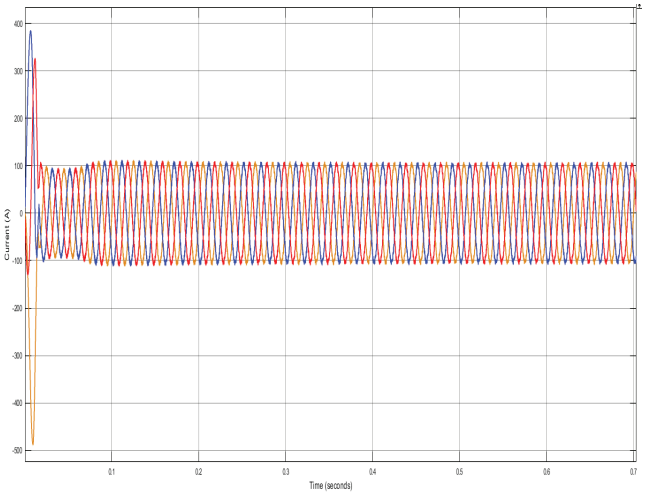

Fig 7 Phase current delivered to grid for irradiance of 1000 W/m2

Fig. 7 shows the phase current delivered by the inverter to the grid for irradiances of 1000W/m2and fig. 8 is its magnified view whose peak value is around 105 A which is the actual theoretical value that should be flowing to the grid. As seen in the curve, the phase current delivered to the grid regulated by hysteresis band controller is not smooth. It is because we allow certain band limit in the hysteresis band controller. This is done so that the switching losses can be minimized which are quite high for low permissible error/deviation as switching is more frequent. The harmonics can be filtered out of the phase current smoothen it before supplying it to the grid.

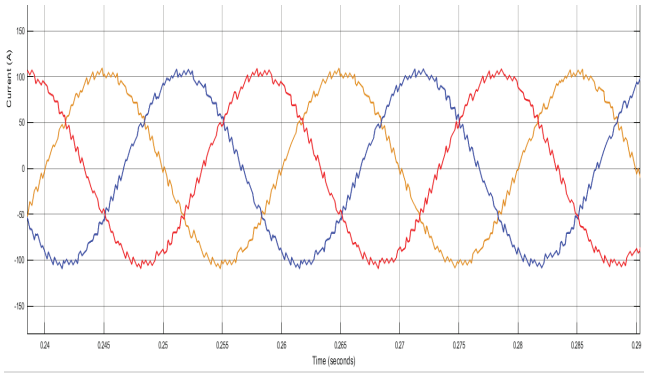

Fig 8 Magnified view of phase current delivered to grid for irradiance of 1000 W/m2

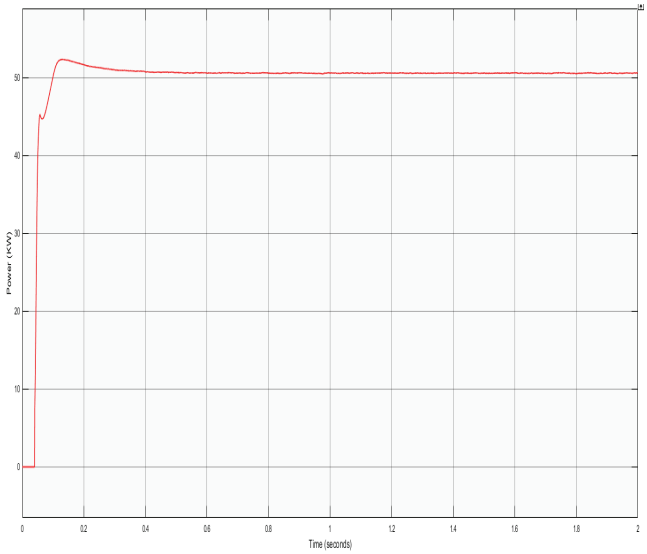

Fig 9 Power delivered to grid for irradiance of 1000 W/m2

Fig. 9 shows the active power delivered to the grid for irradiances of 1000W/m2. At steady state, the power delivered is around 51 KW which is equal to the value observed.

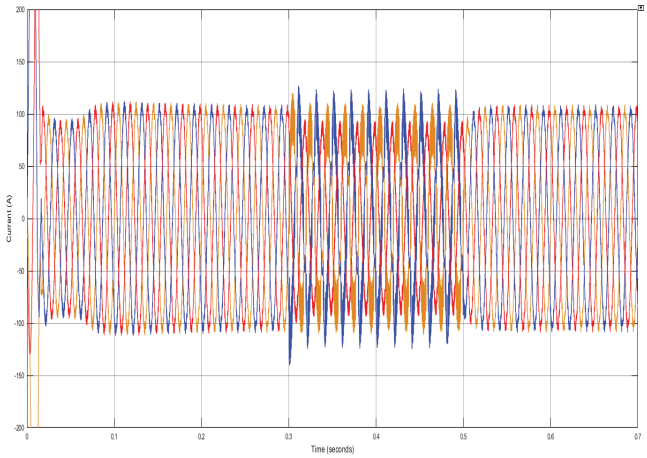

Fig 10 Phase current flowing through the inverter for unbalanced load at the inverter side between 0.3-0.5 sec.

Fig. 10 depicts the phase current flowing through the inverter for the unbalanced load at the inverter side between 0.3-0.5 second. We can see that the current supplied by the inverter remains doesn't fluctuate much as portion of current goes to grid as well as unbalance load during unbalanced loading condition.

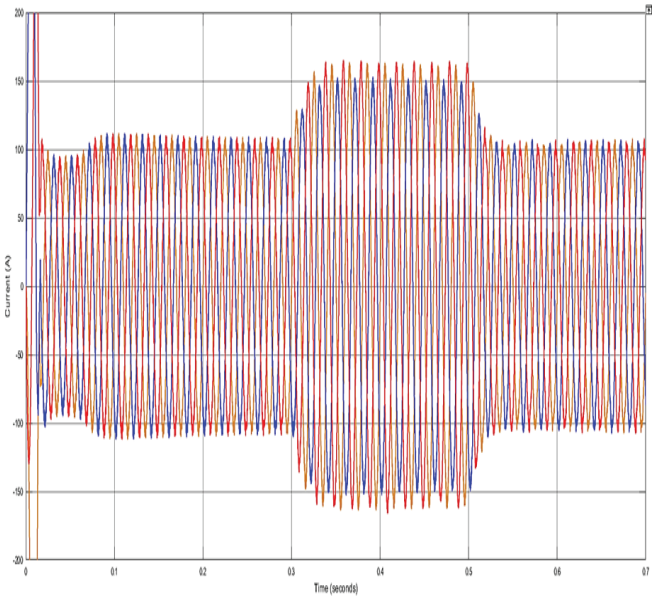

Fig 11 Phase current flowing through the inverter for the unbalance fault at the grid side between 0.3-0.5 sec.

Fig. 11 shows the phase current flowing through the inverter for unbalance fault at grid side between 0.3-0.5 sec. The inverter supplies the rated value of current to the grid during normal condition while the current increases by around 50 A during fault condition. The rise in current isn't much though the fault current flowing through the faulty section is too high. It is because of the fact that majority of fault current is supplied by the load.

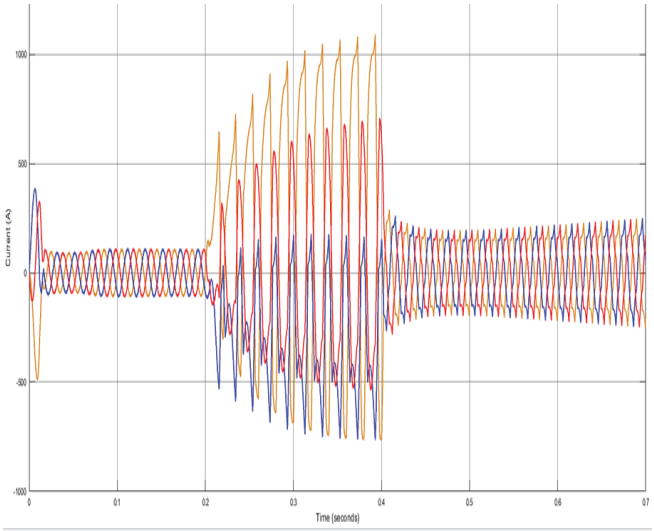

Fig 12 11 Phase current flowing through the inverter for the unbalance fault at the inverter side between 0.3-0.5 sec.

Fig. 12 shows the phase current flowing through the inverter. Before fault occurs, the inverter supplies the rated value of current i.e., 105A. During fault conditions of duration 0.2 sec, the inverter current rises significantly to around 1000A. This high current flowing through the inverter may damage the inverter. The current decreases suddenly and again start rising slowly leading a instability issue even after the fault has been cleared.

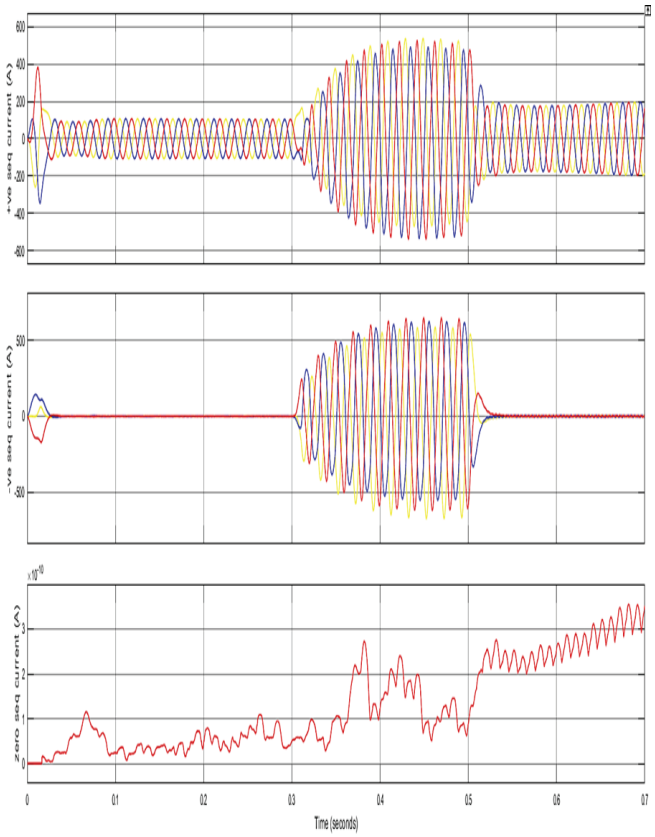

Fig 13 +ve,, -ve and zero sequence components of current flowing through the inverter for the unbalance fault at the inverter side between 0.3-0.5 sec.

Fig. 13 depicts the phase current flowing through the grid in terms of sequence components of current. At normal condition, there is the existence of positive sequence component of current equivalent to the rated value of current that should be delivered by the inverter to the grid while negative and zero sequence current are zero. After the LG fault occurs at the inverter side for a duration of 0.2 sec, there is fluctuation in the positive sequence of current as the inverter has to supply the current to the faulted line and there is also a mutual sharing to the load both by the inverter and the grid. And there is also increase in the both negative and zero sequence component of current. After the fault has been cleared, the negative and zero sequence current becomes zero but the positive sequence current increases to a high value and it goes on increases due to stability issue.

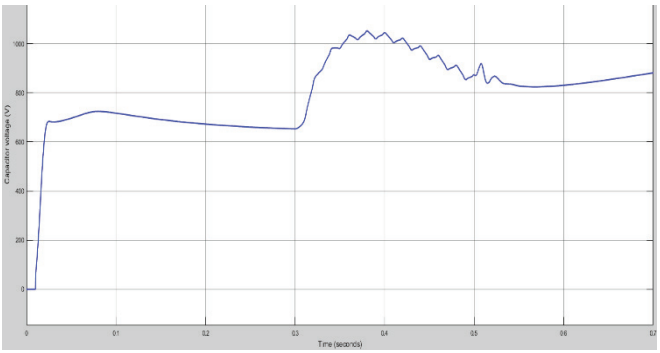

Fig14 Voltage across the dc link capacitor for the unbalance fault at the inverter side between 0.3-0.5 sec

Fig. 14 depicts the voltage across the dc link capacitor. It is observed that the capacitor voltage rises toa round 1050 V from around 640 V. This high voltage may damage the capacitor and often required high rating of capacitor. And the capacitor voltage doesn't settle down to its rated value even after the fault has been cleared, it goes on increasing.

TABLE 2

COMPARISON OF CURRENT FLOWING THROUGH THE INVERTER AND VOLTAGE ACROSS THE DC LINK CAPACITOR AT DIFFERENT FAULT CONDITION

Disturbance Type	**Current flowing through the inverter(A)**				**Capacitor Voltage (V)**
	+ve sequence	***-ve sequence***	***Zero sequence***	***Total***	
Normal condition	105	0	0	105	640
Unbalance load at inverter side	95	13	0	120	630
LG fault at grid side	155	5	0	160	655
LG fault at inverter side	550	600	0	950	1050

❖ *Conclusion obtained from unbalanced load at inverter side*

- Voltage across dc link capacitor doesn't change much.
- Inverter supplies the rated unbalanced load at the inverter side and rest is supplied to the grid.
- Small presence of –ve sequence current and zero sequence current is zero.
- Inverter operation isn't affected by the unbalanced load and is safe.

❖ *Conclusion obtained from unbalanced fault at grid side*

- Majority of the fault current is delivered by the grid and slight increase in the current flowing through the inverter if fault occurs at the grid side.

- No presence of –ve and zero sequence components in the current flowing through the inverter.
- Both –ve and zero sequence components of current is supplied by the grid.
- Voltage across the dc link capacitor changes within the permissible limit.

❖ *Conclusion obtained from unbalanced fault at inverter side*

- Voltage across the dc link capacitor increases during LG fault.
- Majority of the fault current is delivered by the inverter and partially by the grid when fault occurs at the inverter side which may damage the inverter.
- There occurs a stability problem when fault period exceeds 0.08 sec (where current passes above 800A).
- -ve sequence component exists in both the current flowing through the inverter and the grid.
- All the zero-sequence current is supplied by the grid.

B. Observations of Proposed system

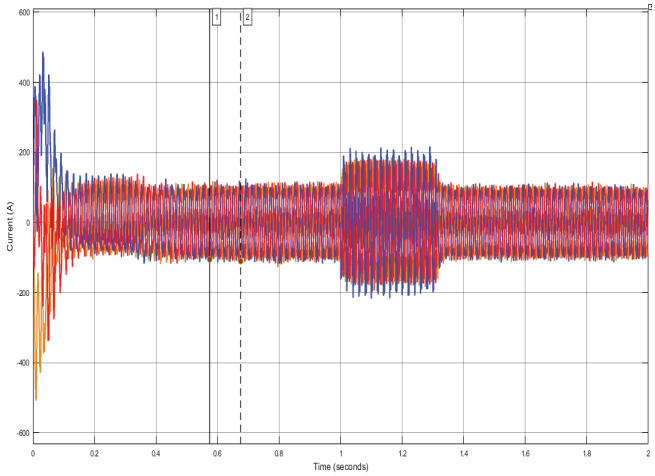

Fig 15 Phase current flowing through the inverter for unbalance fault at the inverter side between 1-1.3 sec after inverter dual current control

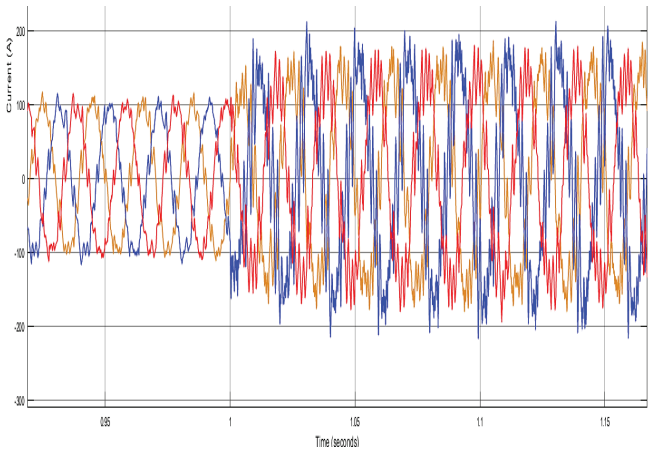

Fig 16 Modified view of phase current flowing through the inverter for unbalance fault at the inverter side between 1-1.3 sec after inverter dual current control

Fig. 15 shows the phase current flowing through the inverter after the replacement of hysteresis controller by the inverter dual current control and fig. 16 is its magnified view. After the replacement of the controller, the current takes slightly larger time to settle down to its rated value in comparison to the hysteresis controller. But during fault condition, the inverter current reduces to around 200 A which is acceptable and prevent the inverter from damages. Also, the inverter current has been settled down to its rated value quickly after the fault has been cleared thereby solving stability issue.

Fig. 17 depicts the phase current flowing through the inverter in terms of its sequence components after the addition of new inverter dual current controller. It is observed that the positive sequence component of inverter current is now reduced to around 150 A from 550 A and the negative sequence current is reduced to almost zero from around 600A during unbalanced fault condition. Thus, the additional inverter dual current controller able to reduce the positive sequence current to an acceptable value and to mitigate the negative sequence current almost completely. The zero-sequence component of current isn't considered in this case as it is being supplied by the grid.

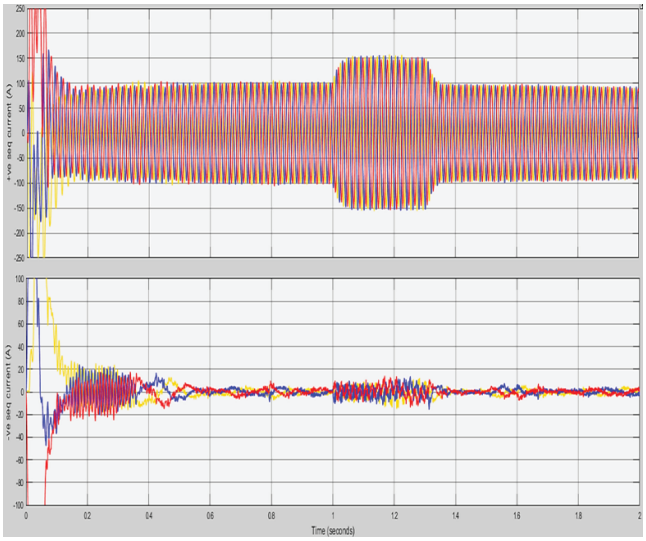

Fig 17 +ve and -ve sequence components of current flowing through the inverter

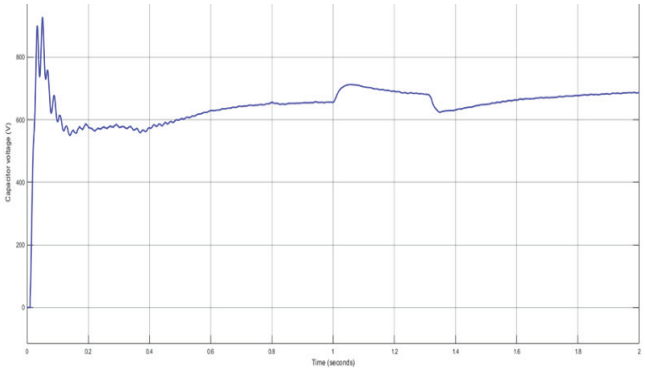

Fig 18 voltage across the dc link capacitor for unbalanced fault at the inverter side between 1-1.3 sec after inverter dual current control

Fig. 18 shows the dc link capacitor voltage waveform after the addition of new inverter dual current controller replacing the hysteresis band controller. The capacitor voltage now limits to around 700V from 1050V during the fault condition. And the voltage settles down to its rated value of around 640V after the fault has been cleared thus solving the stability issue and preventing the capacitor from damages.

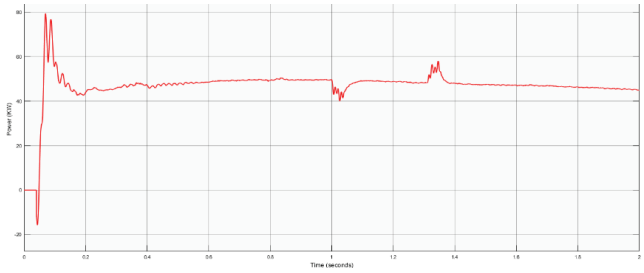

Fig 19 Active power flowing through the inverter for unbalanced fault at the inverter side between 1-1.3 sec after compensation

Fig. 19 shows the active power flowing through the inverter after addition of inverter dual current controller. During faulty period i.e., from 1s to 1.3s the power flowing through the inverter is equal to power flowing through the inverter in normal operating condition. Thus, our designed inverter module is able to supply constant power even during unbalance load and fault condition.

TABLE 3

COMPARISON OF RESULT BEFORE AND AFTER COMPENSATION FOR UNBALANCE FAULT AT THE INVERTER SIDE

Type of controller		Current flowing through the inverter (A)				Capacitor Voltage (V)
		+ve seq.	-ve seq.	Zero seq.	Total	
Before compensation	Hysteresis band controller	550	600	0	950	1050
After compensation	Inverter dual current control	150	10	0	200	700

Conclusions

The problems caused by the unbalanced load and unbalanced fault condition is studied in grid tied PV connected inverter using hysteresis band control in MATLAB Simulink. The unbalanced fault at the inverter side is found to be more severe causing high value of current flowing through the inverter and increase in voltage of dc link capacitor affecting the stability of system. An inverter dual current control is introduced into the system replacing hysteresis band controller such that the current flowing through the inverter is limited from 950A to 200A and voltage across the dc link capacitor is limited to 700V from 1050V during LG fault at the inverter side. So, both current and voltage are limited to a tolerable value and it also addresses the stability issue ensuring safe and reliable operation of the inverter.

References

[1] A. M. Lede, M. G. Molina, M. Martinez, and P. E. Mercado, “Microgrid architectures for distributed generation: A brief review,” 2017 IEEE PES Innovative Smart Grid Technologies Conference - Latin America, ISGT Latin America 2017, vol. 2017-Janua, pp. 1–6, 2017.

[2] N. K. T. S. P. K. B. R. S. T. S. Ashwin Kumar Devarakonda, "A Comparative Analysis of Maximum Power Point Techniques for Solar Photovoltaic Systems," in *Energies 2022*, 2022.

[3] A. A. M. Sarvi, "A comprehensive review and classified comparison of MPPT algorithms in PV systems," Energy Syst, pp. 281-320, 2021.

[4] P. M. N. G. P.K. Atri, "Comparison of Different MPPR Control Strategies for Solar Charge Controller," pp. 65-69, 2020.

[5] P. I. Chtouki, "Comparison of Several Neural Network Perturb and Observe MPPT Methods for Photovoltaic Applications," pp. 909-914, 2018.

[6] S. H. D. K. J. R. M. Khosravi, "A Novel Hybrid Model -Based MPPT Algorithm Based on Artificial Neural Networks for Photovoltaic Applications," pp. 1-6, 2017.

[7] Q. Zhong, “Robust Droop Controller for Accurate Proportional Load Sharing Among Inverters Operated in Parallel,” IEEE Transactions on Industrial Electronics., vol. 60, no. 4, pp. 1281-1290, 2013.

[8] Y. Li, D. M. Vilathgamuwa, P. C. Loh. “Microgrid power quality enhancement using a three-phase four-wire grid-interfacing compensator,” IEEE Transactions on Industry Applications., vol. 41, no. 6, pp. 1707-1719, 2005.

[9] M. Z. Kamh and R. Iravani, “Unbalanced model and power flow analysis of microgrids and active distribution systems,” IEEE Trans. Power Del., vol. 25, no. 4, pp. 2851-2858, Oct. 2010.

[10] H. S. Song and K. Nam, “Dual current control scheme for PWM converter under unbalanced input voltage conditions,” IEEE Transactions on Industrial Electronics, vol. 46, no. 5, pp. 953–959, 1999.

[11] F. Shahnia, R. Majumder, A. Ghosh, G. Ledwich, and F. Zare, “Operation and control of a hybrid microgrid.

[12] K. Ge, Z. Fan, L. Fang and J. Chen, "Inverter Control Based on Virtual Impedance Under Unbalanced Load," in *2020 IEEE 29th International Symposium on Industrial Electronics (ISIE)*, 2022.

[13] Y. Yang, A. Sangwongwanich, H. Liu, and F. Blaabjerg, "Low voltage ride-through of two-stage grid-connected photovoltaic systems through the inherent linear power-voltage characteristic," in Applied Power Electronics Conference and Exposition (APEC), 2017 IEEE, pp. 3582-3588,2017.

[14] W. U. Tareen, S. Mekhilef, M. Seyedmahmoudian, and B. Horan, “Active power filter (APF) for mitigation of power quality issues in grid integration of wind and photovoltaic energy conversion system,” Renew. Sustain. Energy Rev., vol. 70, no. December 2016, pp. 635–655, 2017.

[15] A. D. S. A. S. T. Y. S. Saurav Roy Choudhury, "Adaptive shunt filtering control of UPQC for increased nonlinear loads," *IET Power Electronics,* 2019.

[16] V. R. Chowdhury and J. W. Kimball, "Control of a Three-Phase Grid-Connected Inverter Under Non-Ideal Grid Conditions With Online Parameter Update," *IEEE,* vol. 34, pp. 1613 - 1622, 2019.

[17] P. Shah and B. Singh, "Adaptive Observer Based Control for Rooftop Solar PV System," *IEEE,* vol. 35, pp. 9402 - 9415, 2020.

[18] H. Jiang, H. Pan and B. Shang, "An individual sequencing control strategy for three-phase four-leg inverter under unbalanced loads - ScienceDirect," in *Energy Reports*, 2022.

[19] D. Soto, C. Edrington, S. Balathandayuthapani, and S. Ryster, "Voltage balancing of islanded microgrids using a time-domain technique," Electr. Power Syst. Res., vol. 84, no. 1, pp. 214–223, 2012.

[20] P. K. Goel, B. Singh, S. S. Murthy, and N. Kishore, "Isolated wind-hydro hybrid system using cage generators and battery storage," IEEE Trans. Ind. Electron., 2011.

[21] H. C. Chen, C. T. Lee, P. T. Cheng, R. Teodorescu, and F. Blaabjerg, "A Low-Voltage Ride-Through Technique for Grid-Connected Converters with Reduced Power Transistors Stress," IEEE Trans. Power Electron., 2016.

[22] P. V. PATEL, "MODELING AND CONTROL OF THREE-PHASE GRID-CONNECTED PV," pp. 29-31, 2018.